Cumhuriyet Sci. J., 45(2) (2024) 352-359
DOI: https://doi.org/10.17776/csj.1351460

Cumhuriyet Science Journal

| csj.cumhuriyet.edu.tr | Founded: 2002 ISSN: 2587-2680 e-ISSN: 2587-246X Publisher: Sivas Cumhuriyet University

Polydopamine-mediated facile Silver grown on ZnO Thin Films as High Performance SERS Substrates for R6G Detection

Sami Pekdemir [1,2,a,*]

[1] *Department of Aeronautical Engineering, Faculty of Aeronautics and Astronautics, Erciyes University, Kayseri, 38039,Türkiye.*
[2] *ERNAM - Erciyes University Nanotechnology Application and Research Center, Kayseri, 38039, Türkiye.*
**Corresponding author*

Research Article

History
Received: 28/08/2023
Accepted: 30/05/2024

This article is licensed under a Creative Commons Attribution-NonCommercial 4.0 International License (CC BY-NC 4.0)

ABSTRACT

Surface-enhanced Raman spectroscopy (SERS) is a widely known technique that uses plasmonic structures (silver, gold, etc.) to detect low-concentration molecules. However, the limited number of metallic elements with plasmonic properties leads to limitations in their application. The qualitative detection method of SERS holds considerable promise in providing novel platforms for diverse applications, owing to its utilization of hybrid structures. Mussel-inspired polydopamine offers a promising avenue for the fabrication and integration of hybrid structures suitable for the SERS platform. Here, sputtered ZnO thin films were modified with Ag Nanostructures using polydopamine to fabricate a homogeneous Ag@ZnO hybrid high-performance SERS substrate. Ag/ZnO hybrid nanostructures were analyzed by FESEM and XRD to investigate their morphological and structural characterizations. SERS measurements were performed for all silver growth times to understand the effect of the silver growth process and hybrid structure synergy on SERS performance. The Ag@ZnO hybrid structure, cultivated with 24-hour silver growth, exhibited remarkable detectability even at an ultra-low R6G concentration of 10 pM.

Keywords: Polydopamine, Plasmonics, SERS, Ag-ZnO hybrid structures, R6G.

[a] *samipekdemir@erciyes.edu.tr* *https://orcid.org/0000-0002-7929-6849*

Introduction

Surface-Enhanced Raman Spectroscopy (SERS) has emerged as a powerful analytical technique for enhancing the vibrational signals of molecules adsorbed onto metallic surfaces [1]. To further harness the potential of SERS for sensitive and selective molecular detection, the design and fabrication of high-performance SERS substrates are of paramount importance [2]. Among various materials, zinc oxide (ZnO) thin films have attracted attention due to their unique optical and chemical properties, making them promising candidates for SERS applications [3]. Moreover, the incorporation of silver (Ag) nanostructures onto ZnO surfaces can significantly amplify the SERS signal through the localized surface plasmon resonance effect [4]. Achieving controlled Ag nanostructure growth on ZnO substrates, however, remains a challenge [5].

In recent years, the design and fabrication of hybrid plasmonic structures has gained prominence as a strategy to unlock even greater SERS sensitivity and reproducibility [6]. Hybrid structures entail the combination of multiple materials with distinct plasmonic properties, synergistically enhancing the overall SERS performance beyond the capabilities of individual components. The incorporation of Ag nanostructures onto other substrates, such as zinc oxide (ZnO) thin films, presents a promising avenue to achieve such enhanced SERS activity.

In this context, the integration of polydopamine (PDA) as a versatile platform for surface modification and metal ion reduction offers a promising avenue for the controlled synthesis of Ag nanostructures on ZnO thin films [7]. PDA, inspired by the adhesive proteins found in marine mussels, exhibits strong adhesion to various substrates and provides functional groups that facilitate metal ion binding and subsequent reduction [8]. By leveraging the inherent properties of PDA, a facile approach to the controlled growth of Ag nanostructures on ZnO thin films becomes feasible, thereby enhancing the SERS activity of the resulting substrates.

In this study, we delve into the innovative strategy of utilizing PDA-assisted Ag growth on ZnO thin films to fabricate high-performance SERS substrates. ZnO thin films are fabricated through a diverse array of techniques, encompassing RF/DC magnetron sputtering, chemical vapor deposition (CVD), pulsed laser deposition (PLD), organic vapor phase epitaxy (MOVPE), molecular beam epitaxy (MBE), and sol-gel methods [9]. Notably, RF/DC magnetron sputtering facilitates precise manipulation of chemical composition and deposition rates. Additionally, its execution within a high-vacuum environment ensures the creation of thin films characterized by high purity, homogeneity, and exceptional quality. The introduction of surface-bound Ag nanostructures (Ag NSs) onto ZnO thin films was accomplished through the incorporation of polydopamine, inspired by the adhesive properties of mussels [7]. Polydopamine's solution-phase deposition confers flexibility to surface functionalization and

provides the requisite chemical groups for Ag ion reduction. The evaluation of Ag NS size and structure variations due to growth conditions was conducted through field emission scanning electron microscopy (FESEM) imaging. The collaborative effect of PDA-mediated Ag growth and ZnO thin films facilitated the sensitive detection of the R6G analytical molecule, achieving a remarkable detection limit of 10 pM.

Experimental

Materials

Silicon wafers (<100>, N/Phos) were purchased from Wafer World Inc. ZnO sputtering target (99.999% purity, 2 inch diameter) was purchasing from Plasmaterials inc. Dopamine hydrochloride (Sigma H8502), Tris-EDTA buffer solution, $AgNO_3$ salt and Rhodamine 6G (R6G) was purchased from Sigma-Aldrich. Ethanol, was purchased from Merck.

Deposition of ZnO thin Film on Si substrate Fabrication

RF magnetron sputtering was used to deposited ZnO thin films on a Si (100) substrate using the NANOVAK NVTS-400. Fabrication of ZnO films was done using a ZnO target and argon gas (99.999% purity). Si (100) substrates were cleaned with an ultrasonic cleaner using acetone, isopropyl alcohol, ethanol, and dried by blowing nitrogen gas, respectively. After the drying process was completed, the samples were cleaned in vacuum with O_2 plasma system at 15 W power for 10 minutes in order to clean the surface from hydrocarbon residues and for better adhesion of the thin film to the surface. Before to starting the thin film deposition process, the chamber was purged down to a base pressure of $2x10^{-6}$ Torr. Under 3.9 mTorr pressure, 15 sccm argon flow rate, 80 W RF power, and room temperature conditions, thin films were deposited. ZnO thin films with a thickness of 250 nm were deposited at a rate of 0.3 /s. During the growing process, the ZnO films thickness and growth rate were measured using the QCM thickness measuring equipment (Inficon).

Polydopamine-mediated in situ growth of Ag nanostructures on sputtered ZnO thin film

Mussel inspired Polydopamine (PDA) thin film coating on Si (100) substrates ($1x1cm^2$) with a 250 nm thick ZnO film. The substrates were submerged in a dopamine solution for 30 minutes (1 mg/mL in 5 mM Tris-EDTA buffer, pH 8.5) at room temperature. After coating with PDA, the samples were rinsed with distilled water and dried with N_2 gas. The PDA coated substrates were then treated in steady state with silver nitrate solution (50 mM $AgNO_3$ in 5 mL distilled water) at steady state for various Ag growth times (12, 24, and 36 hours).

Characterization of ZnO thin films and Ag@ZnO substrate

The morphology of the substrate was analyzed by scanning electron microscopy (SEM) imaging that was performed at 3 kV (FESEM, Zeiss Gemini 500). X-ray diffraction patterns of silver decorated ZnO thin film hybrid nanostructures (Ag@ZnO) were analyzed by Grazing Incidence X-ray Diffraction (GIXRD) technique in the range of 30^o-85^o 2θ on a Panalytical X-ray diffractometer.

SERS Measurements of Ag decorated ZnO thin films

Plasmonic properties of the Ag@ZnO was investigated by Raman spectroscopy. An analyte molecule dropped Ag@ZnO samples with various silver growth time was performed Raman measurement which called SERS. The SERS activity of the Ag-structured ZnO film was systematically investigated utilizing a confocal Raman microscope (Alpha M+, Witec, Germany), which was equipped with a 532 nm laser. The experimental setup involved the drop-casting of an aqueous solution of Rhodamine 6G (R6G) onto both the unmodified and Ag-decorated ZnO films, wherein the Ag decoration was accomplished via a PDA coating. Unless explicitly specified, a consistent volume of 2 µL and concentration of 100 µM for the R6G solution were maintained. Raman measurements were conducted post the complete evaporation of the water. The acquisition of Raman spectra employed a 100× objective featuring a numerical aperture value of 0.9. The spectral acquisition time was set at 0.05 s, and the laser power was maintained at 0.1 mW.

To map the SERS activity of the surfaces, a spatial resolution of 0.5 µm was employed, encompassing a 40 × 30 μm^2 area. This mapping relied on the distinctive peak of R6G, with the aromatic C–C stretch peak at 1361 cm^{-1} serving as the characteristic marker. The intensity of this peak facilitated both Raman mapping and determination of the detection limit.

To ascertain the limit of detection, the concentration of R6G was systematically varied from 1 µM down to 10 pM. A stock solution of R6G at a concentration of 10 mM was initially prepared, and subsequent lower concentrations were obtained through dilution with deionized water. Each solution, with a volume of 2 µL, was subsequently deposited onto the SERS substrate, and Raman measurements were conducted post evaporation of the water. In this limit of detection investigation, SERS spectra were recorded from a minimum of 10 distinct locations, with each acquisition lasting for 0.1 s.

Results And Discussion

Figure 1 provides a schematic representation of the key stages and outcomes involved in the production of ZnO thin films and the subsequent development of Ag nanostructures on these surfaces.

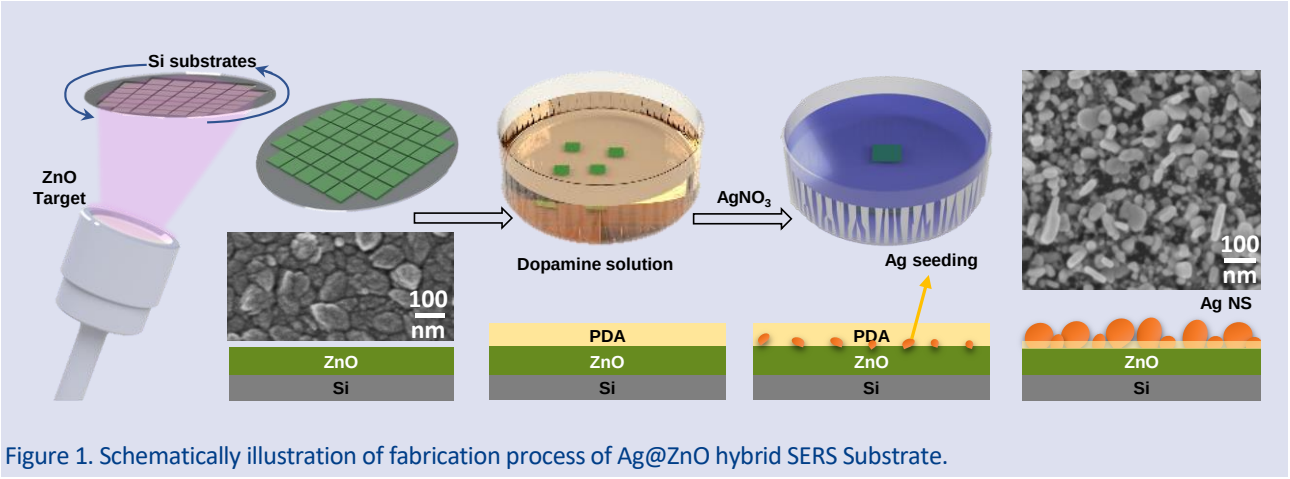

Figure 1. Schematically illustration of fabrication process of Ag@ZnO hybrid SERS Substrate.

Initially, Si substrates, cut into 1x1 cm² dimensions, were meticulously cleaned using acetone, propanol, and ethanol. These square-shaped Si samples were then introduced into the vacuum thin film system. Once the vacuum pumps-initiated operation, the system awaited the attainment of a starting pressure of $3x10^{-7}$ Torr. The coating process commenced by introducing high-purity Ar gas into the system, followed by the activation of the RF power unit to generate plasma. Subsequently, the target material underwent preliminary cleansing via plasma treatment, effectively removing potential contaminants before they could reach the sample surface.

Following this pre-cleaning step, the actual coating process was initiated. This involved opening the shutter positioned in front of the sample and resetting the thin film thickness gauge. As the thickness reading reached 250 nm on the thin film thickness meter system, the cover automatically closed to maintain a consistent film thickness. Once the coating process was complete, the system was halted by deactivating the RF power supply and gas flow, and the sample was extracted from the vacuum environment by introducing gas into the system.

The Si/ZnO samples, now withdrawn from the system, were immersed in a freshly prepared dopamine solution with a pH value of 8.5. These samples were then kept in darkness for a duration of 30 minutes. During this period, the dopamine molecules polymerized in response to the basic environment, resulting in the formation of a PDA thin film on the Si/ZnO sample.

Subsequently, the PDA-coated sample underwent immersion in a 50 mM $AgNO_3$ solution for varying durations (12, 24, and 36 hours) to facilitate the growth of Ag nanostructures. Leveraging the inherent capability of PDA to catalyze the reduction of metallic ions, an observable reduction process occurred. This transformation involved the conversion of dissolved silver ions through interaction with the PDA thin film.

The topological and structural characteristics of Ag-grown ZnO (Ag@ZnO) hybrid structures were investigated through scanning electron microscopy (SEM) imaging. Figure 2 illustrates the influence of the silver growth mechanism on the surface topology of the ZnO thin film.

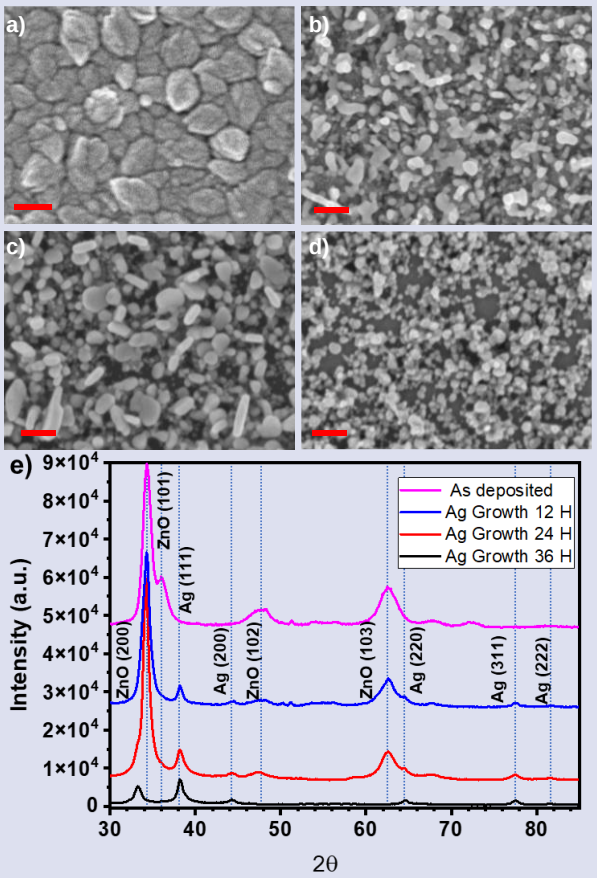

Figure 2. SEM images (scale bar: 100 nm) and XRD measurement. a) SEM image of ZnO thin film as deposited. b) SEM image of Ag@ZnO hybrid structures after 12 h Ag growth. c) SEM image of Ag@ZnO hybrid structures after 24 h Ag growth. d) SEM image of Ag@ZnO hybrid structures after 36 h Ag growth. e) XRD results of the ZnO and Ag@ZnO hybrid structures.

Figure 2a presents an SEM image of the as-deposited ZnO thin film. The ZnO film exhibited high uniformity, devoid of any discernible cracks, and was composed of nanoscale grains. Following the growth of silver, the surface morphology underwent a significant transformation, resulting in the formation of small silver nanoparticles. Notably, in the absence of the PDA coating, noteworthy silver growth was not observed. The growth

of Ag nanostructures on the surface was facilitated through a mussel-inspired PDA thin film.

Morphology was systematically investigated for variations in the substrate in response to different Ag deposition periods. The growth duration exerted a direct influence on the dimensions of the Ag nanostructures (Ag NSs). During a 12-hour growth interval, the production of Ag NSs was incomplete, and their dimensions predominantly remained below 25 nm. However, extending the growth period to 24 hours yielded the development of Ag NSs ranging in size up to 100 nm, excluding those exceeding 50 nm. Subsequently, with a further extension to a 36-hour growth period, the average Ag NS size reduced to 20 nm. This reduction in size is plausibly attributed to potential deterioration of the underlying ZnO film within the aqueous growth solution. It is noteworthy that particles dislodged from the surface were observed in the wastewater subsequent to the growth process termination. Consequently, particles became discernible in the rinse water of the substrate, implying a separation of particles from the surface. The substantiation for this deduction is reinforced by EDX results (Table 1), which exhibit variations in the silver content within the sample (as seen in Figure 3). Notably, the Ag NS-decorated samples showcase consistent Si content. The utilization of normalized EDX counting enables a comparative analysis of element quantities across the samples. Over the course of the silver growth process, the silver content exhibited a gradual increment, culminating in its peak value at the 24-hour growth rate. However, this content exhibited a decline at the 36-hour interval, presumably due to weathering effects.

Table 1. Elemental composition of the Samples.

Samples	% Atomic Si	% Atomic O	% Atomic Zn	% Atomic Ag
ZnO	20.59402	35.63005	43.77593	0
Ag(12h)@ZnO	33.01004	33.4837	21.07815	12.4281
Ag(24h)@ZnO	35.59322	28.66468	13.62803	22.11406
Ag(36h)@ZnO	34.40178	36.51642	13.98998	15.09182

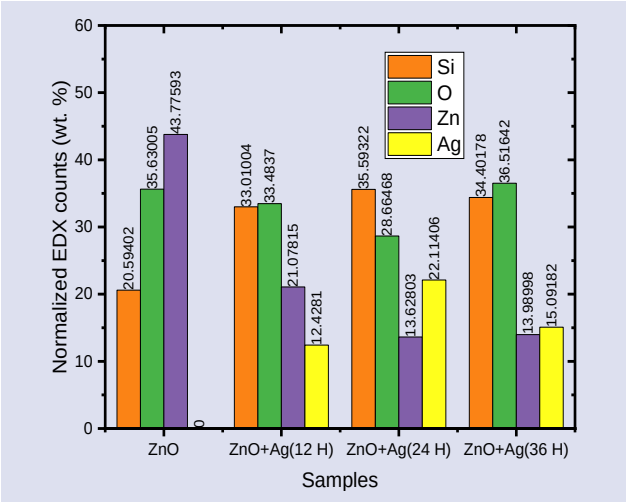

Figure 3. Elemental analyses of Samples by normalization EDX counts

The formation of Ag NSs on the ZnO film can be rationalized through the metal ion reduction capabilities of PDA. Notably, the absence of PDA prevented the development of Ag nanostructures on the ZnO layer (see figure 4). This observation underscores the essential role of functional groups introduced by PDA in facilitating the surface growth of Ag NSs.

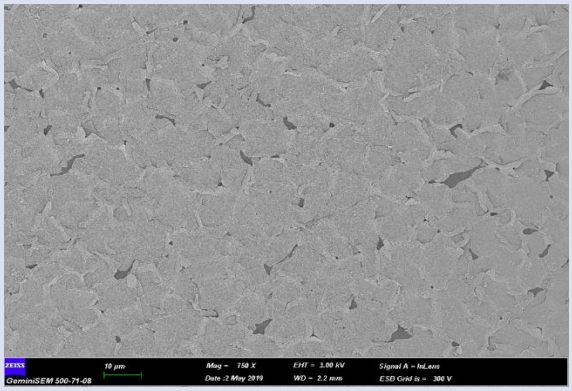

Figure 4. SEM image of decomposed ZnO thin film after the Ag growth process without PDA coating

The diffraction data were acquired through X-ray diffraction (XRD), alongside quantitative analysis. The XRD patterns of both the ZnO thin film and Ag-modified samples, obtained for various Ag growth durations, are depicted in Figure 2.e. The presence of diffraction peaks at 34.5° and 62.6° corresponding to the (200) and (130) crystallographic planes, respectively, substantiates that the ZnO films exhibit excellent agreement with the wurtzite hexagonal crystal structure (JCPDS No. 36-1451) [10]. The peak at 36.1° can be attributed to the (101) crystallographic plane [11], which disappeared during the silver growth process. This is the possible result of the water solubility of ZnO [12], as clearly seen in the SEM images of the 36 h silver growth process and discussed in the section on SEM images. Notably, these peaks were absent in the ZnO thin film subjected to a 36-hour growth period, a result attributed to the decomposition of the ZnO underlayer. Furthermore, the diffraction peak at 38.2° corresponds to the (111) plane of the face-centered cubic Ag structure (JCPDS card # 089-3722) [13]. In comparison, the Ag peak intensity on the uncoated PD-modified ZnO film was notably subdued. Additionally, diffraction peaks corresponding to the (002), (220), (311), and (222) planes, observed at 44.3°, 64.6°, 77.5°, and 81.5°, respectively, can be attributed to silver nanostructures, a direct consequence of the silver growth process.

Optimal peak intensity for both ZnO and Ag was noted in substrates prepared via 24-hour Ag deposition time. The peak intensity of the ZnO (002) plane exhibited an increase with prolonged Ag decoration time. However, after 24 hours, despite the extended Ag decoration period, the intensity of the peak diminished, signifying that adorning Ag for excessive durations disrupts the preferred orientation of ZnO (002).

The average crystallite sizes (D) of the samples were determined utilizing the Debye–Scherrer equation [14]:

$$D = \frac{0.9\times\lambda}{\beta\times\cos\theta} \quad (1)$$

Here, λ, θ, and β represent the wavelength of X-ray radiation, the Bragg's angle of the peaks, and the angular width of peaks at the full width at half maximum (FWHM), respectively. For pure ZnO, the average crystal size was 7.5 nm, exhibiting variations with differing Ag deposition times. Specifically, the average crystallite sizes were 12.55 nm, 13.31 nm, and 11.87 nm for ZnO films decorated with Ag for 12, 24, and 36 hours, respectively. The absence of additional peaks and shifts in peak positions suggests that Ag did not incorporate into the ZnO lattice but remained solely on the surface of ZnO [15].

SEM images and XRD results give us some correlations about the particle sizes (see Figure 5). The particle size analysis shows Ag nanostructures of 13.7 ± 7.6 nm, 15.9 ± 7.8 nm, 10.6 ± 5.1 nm in Ag@ZnO samples with 12, 24, 36 h growth time, respectively. The average particle sizes obtained from SEM images and the crystallite sizes obtained from XRD measurements give comparable results. Based on this correlation, it can be said that the two results support each other and Ag nanostructures are largely composed of single crystal structures.

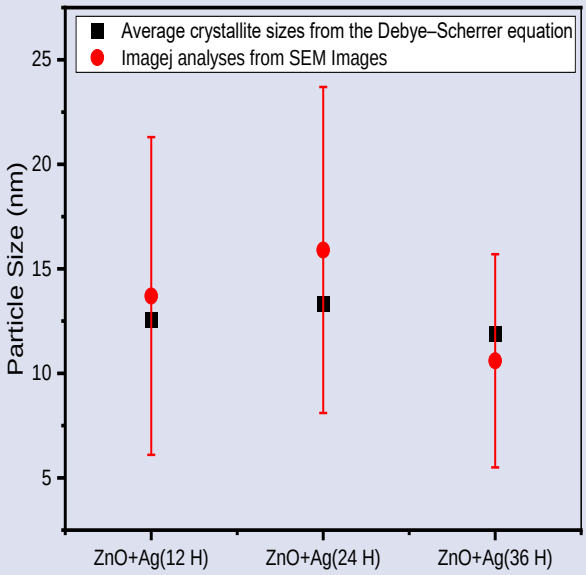

Figure 5. Comparative analysis of average particle sizes obtained from XRD measurement and SEM images

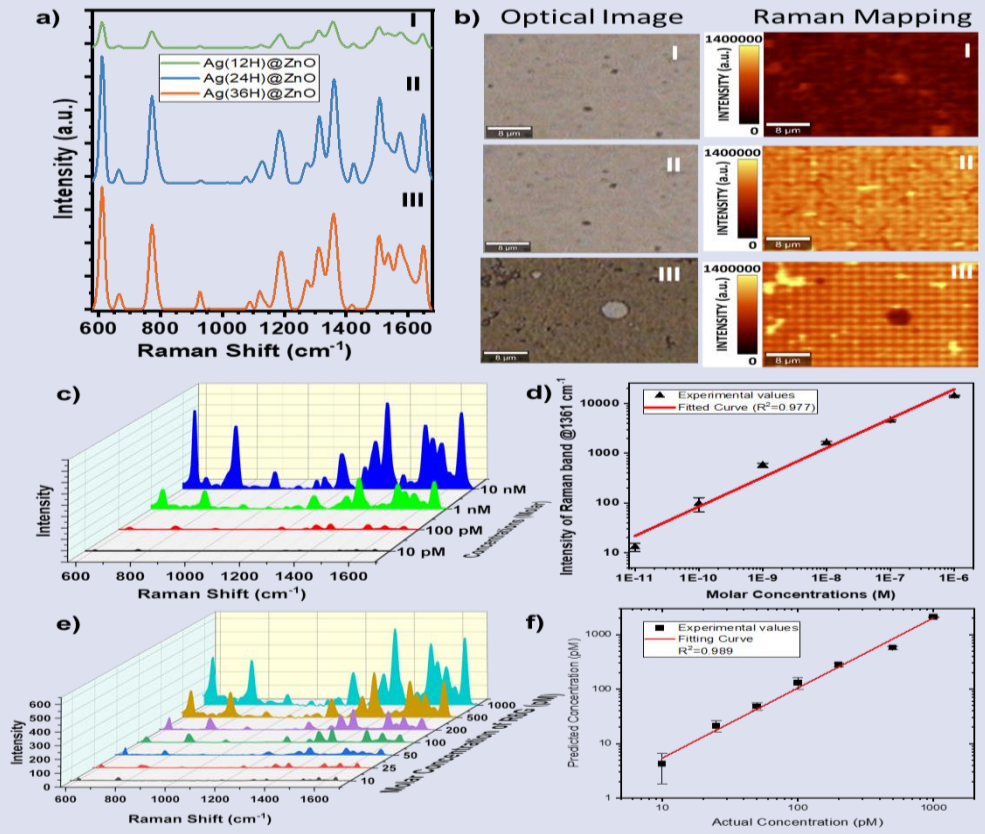

Figure 6. SERS activity of Ag@ZnO nanostructures. a) SERS spectra of R6G on silver decorated ZnO thin films with 12 hours(I), 24 hours(II), 36 hours(III) growth time. b) Optical Images of Raman mapping regions and Raman mapping images of Ag@ZnO with various Ag growth time (12 hours, 24 hours, 36 hours; I, II, III, respectively), obtained by mapping intensities at a Raman shift of 1361 cm^{-1}. c) SERS spectra of R6G at concentrations ranging 10 nM to 10 pM, measured on the Ag(24H)@ZnO. d) Correlation between R6G concentration and SERS intensity at 1361 cm^{-1}. e) SERS measurements were conducted using a distinct set of R6G solutions, spanning concentrations from 1000 pM to 10 pM. f) Calculated concentrations were predicted using the equation mentioned in section (d) for the aforementioned R6G solution batch.

The SERS activity was explored utilizing Rhodamine 6G (R6G) as a probe molecule. An aqueous R6G solution was drop-cast onto Ag@ZnO samples featuring varying Ag deposition times, and SERS measurements were conducted post-water evaporation. The surface SERS activity was analyzed through the mapping of the characteristic vibrational mode of the probe molecule at 1361 cm^{-1}. This mode originates from the robust C–H in-plane bending of R6G [16]. Among the studied Ag@ZnO samples, noteworthy SERS activity was notably observed in the sample subject to a 24-hour Ag growth period (Ag(24H)@ZnO) (refer to Figure 6.a). The SERS signal intensity at 1361 cm^{-1} from Ag(24H)@ZnO surpassed those from Ag(12H)@ZnO and Ag(36H)@ZnO by factors of 5 and 1.1, respectively.

$$S.D. = \sqrt{\frac{\sum_{i=1}^{n}(x_i-\bar{x})^2}{(n-1)}} \quad (2)$$

$$R.S.D = \frac{\sqrt{\frac{\sum_{i=1}^{n}(x_i-\bar{x})^2}{(n-1)}}}{\frac{\sum_{1}^{n} n}{n}}.100 \quad (3)$$

Here; x_i is i labeled data, $\bar{x}$ is average of all data sets, n is number of all data sets.

Moreover, standard deviation (SD) and relative standard deviation (RSD) values (Table 2) were calculated based on the signal intensities of the 1361 cm^{-1} band using equation (2) and (3), elucidating the substrate efficiency. To calculate the standard deviation, approximately 60 spectra were randomly selected from each mapping image (Figure 7). This comprehensive analysis reveals a commendable level of uniformity across the film, with a 9.3% RSD. The SERS intensity from Ag(24H)@ZnO demonstrates a high degree of uniformity (refer to Figure 8), surpassing that of SERS substrates fashioned from colloidal nanoparticle assemblies [17].

Raman mapping images in Figure 6.b depict the spatial distribution of SERS activity. These images were obtained from Ag@ZnO samples featuring varied Ag growth times (12 hours, 24 hours, 36 hours). Specifically, the mapping images labeled as "I" pertain to Ag@ZnO with a 12-hour silver growth period (Ag(12H)@ZnO). The dark orange Raman mapping image highlights an insufficient AgNS growth for effective SERS activity points, known as "hot-spots". In contrast, the Raman mapping of Ag(24H)@ZnO (II) samples illustrates improved, homogeneous distribution of the SERS signal. While some dark orange and yellow regions persist, the darker orange Raman mapping image for Ag(36H)@ZnO (III) is indicative of Ag nanostructure erosion from the surface, likely connected to the decomposition of the ZnO thin film within the water-based solvent. The occurrence of yellow regions represents aggregated R6G on surface cracks due to decomposing. From these outcomes, it is evident that the most efficient SERS substrate emerges from a 24-hour silver growth process.

Table 2. Statistical analysis of SERS activity on Ag@ZnO samples. S. D. refers to the standard deviation and R. S. D. refers to the relative standard deviation.

Region	Raman Intensity @ 1361 cm^{-1}	S.D.	R.S.D. (%)
Ag(12h)@ZnO	367965	60793	16.5
Ag(24h)@ZnO	1048473	98246	9.3
Ag(36h)@ZnO	1003297	145460	14.5

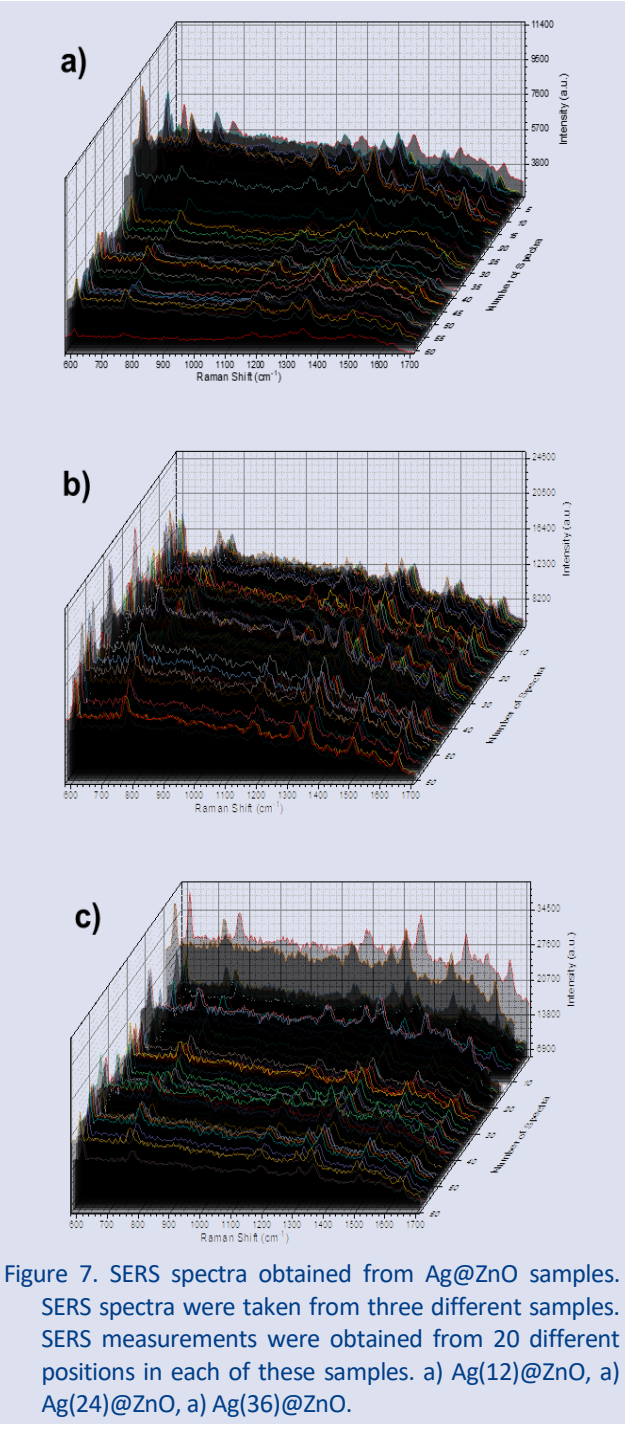

Figure 7. SERS spectra obtained from Ag@ZnO samples. SERS spectra were taken from three different samples. SERS measurements were obtained from 20 different positions in each of these samples. a) Ag(12)@ZnO, a) Ag(24)@ZnO, a) Ag(36)@ZnO.

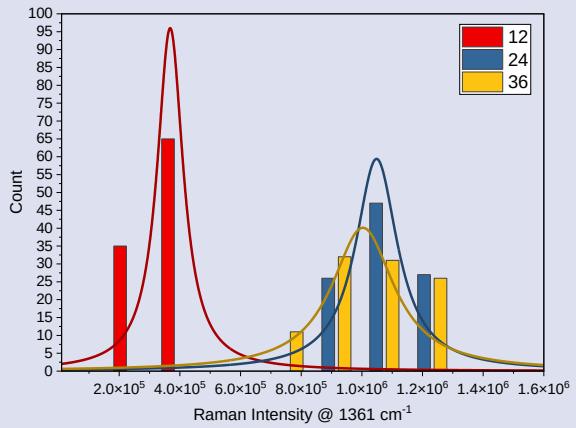

Figure 8. Statistical analysis of SERS activity of Ag@ZnO samples

The limit of detection for SERS-active surfaces represents the lowest detectable concentration through Raman spectroscopy. Raman spectra for varying R6G concentrations (10 nM to 10 pM) are shown in Figure 6.c. The distinct peak of R6G at 1361 cm^{-1} was discernible even at concentrations as low as 10 pM. Overall, the SERS performance of the presented material parallels Ag-ZnO thin film hybrid nanostructures reported in other studies. For instance, in a recent report [15], Ag@ZnO nanoworms were employed as SERS substrates, achieving a detection limit of 100 pM for R6G. In a separate investigation, nanocomposite films were fabricated by cultivating silver nanoparticles on zinc oxide rods[18], which were previously grown on PET substrate using Methenamine. These substrates exhibited surface-enhanced Raman scattering (SERS) detection capabilities, detecting concentrations as low as 100 nM for Malachite green and 1000 pM for p-aminothiophenol. The findings of this study reveal a detection capability that exceeds previous research by a factor of ten or more.

To illustrate the quantitative detection capabilities of Ag(24H)@ZnO, SERS intensity was plotted against the concentration of R6G (Figure 6.d). The resulting curve was well-fitted with the equation , yielding a coefficient of determination (R^2) of 0.981. Furthermore, to underscore the predictive potential of probe molecule concentrations on the presented platform, an additional batch of R6G solutions was prepared, spanning concentrations from 1000 pM to 10 pM. These solutions were then applied to the Ag(24H)@ZnO substrate, and intensity at the 1361 cm^{-1} position was gauged via Raman spectroscopy after water evaporation. Employing the equation derived from the data in Figure 6.d, these intensity values enabled the calculation of solution concentrations. The resultant calculated concentrations represent predicted concentrations and were plotted against actual concentrations (refer to Figure 6.e, 6.f). Notably, a favorable alignment between predicted and calculated concentrations was observed, substantiated by a coefficient of determination (R^2) of 0.989, further affirming the quantitative molecular detection capability of the presented platform.

A quantitative measure of SERS activity is the enhancement factor, which gauges the extent of improvement in Raman scattering intensity relative to a reference substrate. Different enhancement factors have been proposed in the literature [19]. A straightforward definition, known as the analytical enhancement factor (AEF), provides a straightforward and repeatable measurement under predefined conditions [20]. AEF is calculated using the following Eq. (4):

$$\mathrm{AEF} = \frac{I_{SERS}}{I_{RM}} \times \frac{C_{RM}}{C_{SERS}} \quad (4)$$

In this equation, I_{SERS} (13 counts) and I_{RM} (53 counts) denote the intensity of Raman scattering at 1361 cm^{-1} for the SERS and reference substrates, respectively. For the experiments described herein, the reference substrate consisted of an unmodified glass slide. Similarly, C_{SERS} (10 pM) and C_{RM} (10 mM) refer to the solution concentration of the probe molecule for the SERS and reference substrates, respectively. AEF was calculated as 2.45×10^8 for R6G. This enhancement factor of 10^8 is in line with previous reports [15].

Conclusions

In this study, we have successfully fabricated high-performance SERS substrates by cultivating Ag nanostructures with remarkable uniformity on ZnO thin films. The harmonious interplay between PDA-mediated Ag growth and ZnO thin films offers an auspicious avenue for propelling SERS technology forward, bestowing the capability for precise and selective molecular detection across diverse analytical and sensing applications. Inspired by the adhesive prowess of mussels, we have orchestrated Ag@ZnO hybrid structures, fashioning proficient Ag NS configurations on ZnO thin films through the inherent metal ion reduction propensity of the PDA polymer structure. The symbiotic interplay between metal oxide semiconductors and plasmonic metallic nanostructures has engendered the detection of the R6G analyte molecule with an impressive detection threshold reaching 10 pM. In conclusion, this proves a detection capability that surpasses similar efforts in the literature, thus paving the way for promising avenues of future research.

Conflicts of interest

There are no conflicts of interest in this work.

References

[1] K. Kneipp, Y. Wang, H. Kneipp, L.T. Perelman, I. Itzkan, R.R. Dasari, M.S. Feld, Single Molecule Detection Using Surface-Enhanced Raman Scattering (SERS), *Physical Review Letters*. 78 (1997) 1667–1670..

[2] P.L. Stiles, J.A. Dieringer, N.C. Shah, R.P. Van Duyne, Surface-Enhanced Raman Spectroscopy, *Annual Review of*

Analytical Chemistry. 1 (2008) 601–626.

[3] O. Szabó, S. Flickyngerová, T. Ignat, I. Novotný, V. Tvarozek, Gold nanostructures sputtered on zinc oxide thin film and corning glass substrates, *Facta universitatis - series: Electronics and Energetics*. 29 (2016) 77–88.

[4] A. Guerrero-Martínez, S. Barbosa, I. Pastoriza-Santos, L.M. Liz-Marzán, Nanostars shine bright for you, *Current Opinion in Colloid & Interface Science*. 16 (2011) 118–127.

[5] Y. Fang, N.-H. Seong, D.D. Dlott, Measurement of the Distribution of Site Enhancements in Surface-Enhanced Raman Scattering, *Science*. 321 (2008) 388–392.

[6] X.-S. Zheng, I.J. Jahn, K. Weber, D. Cialla-May, J. Popp, Label-free SERS in biological and biomedical applications: Recent progress, current challenges and opportunities, *Spectrochimica Acta Part A: Molecular and Biomolecular Spectroscopy*. 197 (2018) 56–77.

[7] H. Lee, S.M. Dellatore, W.M. Miller, P.B. Messersmith, Mussel-Inspired Surface Chemistry for Multifunctional Coatings, *Science*. 318 (2007) 426–430.

[8] Y. Cong, T. Xia, M. Zou, Z. Li, B. Peng, D. Guo, Z. Deng, Mussel-inspired polydopamine coating as a versatile platform for synthesizing polystyrene/Ag nanocomposite particles with enhanced antibacterial activities, *J. Mater. Chem. B*. 2 (2014) 3450–3461.

[9] M. Kuru, H. Narsat, The effect of heat treatment temperature and Mg doping on structural and photocatalytic activity of ZnO thin films fabricated by RF magnetron co-sputtering technique, *Journal of Materials Science: Materials in Electronics*. 30 (2019) 18484–18495.

[10] H.L. Cao, X.F. Qian, Q. Gong, W.M. Du, X.D. Ma, Z.K. Zhu, Shape- and size-controlled synthesis of nanometre ZnO from a simple solution route at room temperature, *Nanotechnology*. 17 (2006) 3632–3636.

[11] P. Fageria, S. Gangopadhyay, S. Pande, Synthesis of ZnO/Au and ZnO/Ag nanoparticles and their photocatalytic application using UV and visible light, *RSC Adv.* 4 (2014) 24962–24972.

[12] S. Heinonen, J.-P. Nikkanen, E. Huttunen-Saarivirta, E. Levänen, Investigation of long-term chemical stability of structured ZnO films in aqueous solutions of varying conditions, *Thin Solid Films*. 638 (2017) 410–419.

[13] T. Theivasanthi, M. Alagar, Electrolytic Synthesis and Characterization of Silver Nanopowder, *Nano Biomedicine and Engineering*. 4 (2012). doi:10.5101/nbe.v4i2.p58-65.

[14] B.D. Cullity, C.D. Graham, Introduction to Magnetic Materials, *John Wiley & Sons, Inc.*, Hoboken, NJ, USA, 2008.

[15] N.D. Jayram, S. Sonia, S. Poongodi, P.S. Kumar, Y. Masuda, D. Mangalaraj, N. Ponpandian, C. Viswanathan, Superhydrophobic Ag decorated ZnO nanostructured thin film as effective surface enhanced Raman scattering substrates, *Applied Surface Science*. 355 (2015) 969–977..

[16] S. Nie, S.R. Emory, Probing Single Molecules and Single Nanoparticles by Surface-Enhanced Raman Scattering, *Science*. 275 (1997) 1102–1106..

[17] C. Jiang, S. Markutsya, V. V. Tsukruk, Collective and Individual Plasmon Resonances in Nanoparticle Films Obtained by Spin-Assisted Layer-by-Layer Assembly, *Langmuir*. 20 (2004) 882–890.

[18] D. Cheng, Y. Zhang, C. Yan, Z. Deng, X. Tang, G. Cai, X. Wang, Polydopamine-assisted in situ growth of three-dimensional ZnO/Ag nanocomposites on PET films for SERS and catalytic properties, *Journal of Molecular Liquids*. 338 (2021) 116639.

[19] E.C. Le Ru, E. Blackie, M. Meyer, P.G. Etchegoin, Surface enhanced Raman scattering enhancement factors: a comprehensive study, *The Journal of Physical Chemistry C*. 111 (2007) 13794–13803.

[20] Y.C. Kao, X. Han, Y.H. Lee, H.K. Lee, G.C. Phan-Quang, C.L. Lay, H.Y.F. Sim, V.J.X. Phua, L.S. Ng, C.W. Ku, T.C. Tan, I.Y. Phang, N.S. Tan, X.Y. Ling, Multiplex Surface-Enhanced Raman Scattering Identification and Quantification of Urine Metabolites in Patient Samples within 30 min, *ACS Nano*. 14 (2020) 2542–2552.